Potent Cationic Inhibitors of West Nile Virus NS2B/NS3 Protease With Serum Stability, Cell Permeability and Antiviral Activity

Martin J. Stoermer,[†] Keith J. Chappell,[‡] Susann Liebscher,[‡] Christina M. Jensen,[†] Chun H. Gan,[†] Praveer K. Gupta,[†] Wei-Jun Xu,[†] Paul R. Young,[‡] and David P. Fairlie*,[†]

Centre for Drug Design and Development, Institute for Molecular Bioscience, University of Queensland, Brisbane, Queensland 4072, Australia, School of Molecular and Microbial Sciences, University of Queensland, Brisbane, Queensland 4072, Australia

Received May 1, 2008

West Nile virus (WNV) has spread rapidly around the globe, efficiently crossing species from migrating birds into humans and other mammals. The viral protease NS2B-NS3 is important for WNV replication and recognizes dibasic substrate sequences common to other flaviviral proteases but different from most mammalian proteases. Potent inhibitors of WNV protease with antiviral activity have been elusive to date. We report the smallest and most potent inhibitors known for this enzyme, cationic tripeptides with nonpeptidic caps at the N-terminus and aldehyde at the C-terminus. One of these, compound **3** (K_i = 9 nM) is stable in serum (>90% intact after 3 h, 37 °C), cell permeable, and shows antiviral activity (IC_{50} 1.6 μM) without cytotoxicity (IC_{50} >400 μM), thereby validating the approach of inhibiting WNV protease to suppress WNV replication.

Introduction

Viruses with the capacity to cross species and cause fatalities are of major importance to human health and mankind is not well prepared to deal with such emerging threats.[1] In particular, the threat of rapid viral transmission to humans from birds has been seriously underestimated, as highlighted by the speed with which the epidemic of West Nile virus (WNV[a]) has penetrated even developed countries in North America during the past 8 years,[2,3] and by current concerns about the imminent danger posed by avian influenza.[4]

WNV is endemic in the Middle East and parts of Africa but had been associated with relatively unusual infection in humans until recently.[5] Infections are characterized by debilitating illness, severe neurological pathology and fatalities, particularly in the elderly. In the USA alone since 1999, an estimated 280000 illnesses have been attributed to WNV, over 23000 people have presented clinically with WNV infection, and there have been over 900 fatalities.[2] About one-third of patients presenting with infection had encephalitis or meningitis. WNV infection has also killed over 15000 horses and hundreds of thousands of wild and domestic birds. No human vaccine has progressed beyond clinical trials, and there is no effective treatment available for WNV infections.

WNV is one of more than 70 members of the Flavivirus genus[6] that all possess a viral-encoded NS2B/NS3 protease thought to be important for viral replication.[7] It recognizes cleavage sites to the C-terminus of two consecutive basic amino acids in the viral polyprotein precursor and effects post-translational cleavage of this substrate in the cytoplasm of infected host cells to form both structural and nonstructural proteins.[6,7] The WNV NS2B-NS3 enzyme is a serine-like protease that shares structural similarities and substrate preferences with other flavivirus proteases. Inhibitors of proteases in general are proving to be successful treatments for infection by HIV, and inhibitors of serine proteases in particular look promising for treating hepatitis C infections, diabetes, and cardiovascular conditions.[8,9] The WNV NS2B-NS3 serine protease is similarly a possible target for anti-WNV chemotherapy.[10] Importantly, the substrate preferences for two basic residues to the N-terminal side of the putative cleavage site makes this viral serine protease different to most mammalian serine proteases, and this could be a key difference to exploit in designing inhibitors that are selective for this viral protease. Highlighting this point is the fact that WNV NS2B-NS3 is not inhibited by small molecules (e.g., no inhibition by 100 μM PMSF, TLCK, leupeptin, benzamidine, or FUT-175)[11] that are known to be general inhibitors of most human serine proteases. However, the discovery and development of inhibitors for WNV protease has posed significant challenges that have so far not been conquered. Chief among these is the highly anionic nature of the active site substrate-binding groove of the protease resulting in strong preferences for cationic ligands.

Previously, we reported the first catalytically active WNV protease (recombinant NS3 protein fragment tethered at the N-terminus to an essential NS2B cofactor fragment via a nonapeptide linker), developed a valuable functional assay for profiling the enzyme kinetics, and created the first substrate-based inhibitors using a homology model.[11] This led to our investigations of the importance of substrate/cofactor residues using site-directed mutagenesis of the protease and extensive panels of substrates incorporating unnatural amino acids.[12,13] Others have highlighted additional structural features important for function in a crystal structure of the same truncated NS2B-NS3 WNV protease[14] and also reported tetrapeptide inhibitors of micromolar potency against West Nile NS3/NS2B protease.[15] These and other studies on the WNV NS3 protease have

* To whom correspondence should be addressed. For D.P.F.: phone, 617 3346 2989; fax, 617 3346 2990; E-mail, d.fairlie@imb.uq.edu.au. For P.R.Y.: phone, 617 3365 4646; fax, 617 33654620; E-mail, p.young@uq.edu.au.

[†] Centre for Drug Design and Development, Institute for Molecular Bioscience, University of Queensland.

[‡] School of Molecular and Microbial Sciences, University of Queensland.

[a] Abbreviations. DCM, dichloromethane; DIPEA, *N*,*N*-diisopropylethylamine; DMF, *N*,*N*-dimethylformamide; ESMS, electrospray mass spectrometry; NMR, nuclear magnetic resonance spectroscopy; TFA, trifluoroacetic acid; WNV, West Nile virus; pNA, *para*-nitroanalide; PMSF, 4-amidophenylmethanesulfonyl fluoride hydrochloride; TLCK, *N*-tosyl-L-phenylalanine chloromethyl ketone; Nle, norleucine; WNV_{KUN}, west nile virus Kunjin strain.

10.1021/jm800503y CCC: $40.75
Published on Web 08/26/2008

provided valuable information on substrate processing,[11−16] enzyme/cofactor mutagenesis,[12,13,17,18] enzyme structure/function,[12,13,19] catalytic mechanism,[20] and enzyme inhibition[11,21,22] that could potentially help lead to an effective treatment of WNV infection. In particular, information from our previous substrate processing and modeling studies[11−13] has now enabled us to create the first potent peptide-based inhibitors of WNV protease that also display antiviral activity in cells. This study, which includes novel observations of serum stability and cell permeability for cationic peptides containing as few as 2−3 charged amino acids, validates the importance of WNV protease as a putative antiviral drug target. It may also encourage development of NS3 protease inhibitors for combating other members of the Flaviviridae (e.g., dengue fever, yellow fever, hepatitis C, and Japanese/St. Louis/tick-borne/Australian encephalitis) that together place up to three billion people at risk of viral infection.[2]

Results and Discussion

From Substrates to Inhibitors. Previous studies on recombinant NS2B/NS3 proteases of WNV[11−13] and Dengue virus[23,24] suggested that tetrapeptide sequences with *para*-nitroanilide (pNA) or aminomethyl coumarin (AMC) at their C-termini were effective substrates for monitoring protease activity. While the cleavage sites (NS2A-NS2B, NS2B-NS3, NS3-NS4A, NS4A-NS5) in native polypeptide substrates for WNV NS2B-NS3 protease show an invariance of residues at P1 (Arg) and P2 (Lys), a variety of residues are present at P3 (Arg, Thr, Gly, Leu) and P4 (Asn, Tyr, Ser, Gly). A combination of molecular modeling of peptide substrates in the active site of WNV NS2B-NS3 protease, site-directed mutagenesis of protease/cofactor residues, and kinetic data for processing of short peptide substrates featuring unnatural amino acids[12,13] provided us with a better understanding of the importance of S1, S2, S3, and S4 enzyme residues for substrate binding in solution. Thus while Dengue NS2B-NS3 protease prefers Arg at P2, the corresponding WNV protease has a preference for Lys at P2.[12] Those studies resulted in tripeptides such as 2-naphthoyl-KKR-pNA (Km 20 μM) being identified as effective substrates for the WNV protease.[13]

On the basis of those previous studies and some modeling predictions reported here, a range of tripeptide substrates have now been converted into aldehyde derivatives (X-KKR-aldehyde; Figure 1, Table 1) to prospectively inhibit the protease. In particular, we decided to focus on mapping the space at the N-terminus of these peptides (X) in order to test whether substituents at this position could enhance interaction with enzyme. Initial results are shown in Figure 1 for a panel of compounds tested as potential inhibitors of the processing of tetrapeptide substrate AcLKKR-*p*NA by WNV protease at a single concentration (10 μM).

Several compounds were found to inhibit WNV protease activity by >80% (e.g., **1**−**3, 10**, **20**, **21**, **23**) at this concentration, and they were subsequently examined in dose-dependent experiments to obtain IC_{50} values (Table 1). The structures of the N-terminal capping motifs (see Supporting Information) in compounds **1**−**28** suggest that some degree of flexibility rather than rigidity at this position confers more potent inhibition. Thus compounds **3**, **10**, **20**, and **21** with flexible phenacetyl substitutents were most effective, while urea (**23**) and carbamate (**24**) linkages were well tolerated in inhibitors. We also prepared four derivatives (**25**−**28**) with more and less flexibility in the chain connecting the aromatic residue to the P3 lysine while incorporating an oxygen atom at the benzylic position.

To ascertain whether aldehyde inhibitor potency absolutely required the three basic residues, a small panel of inhibitors

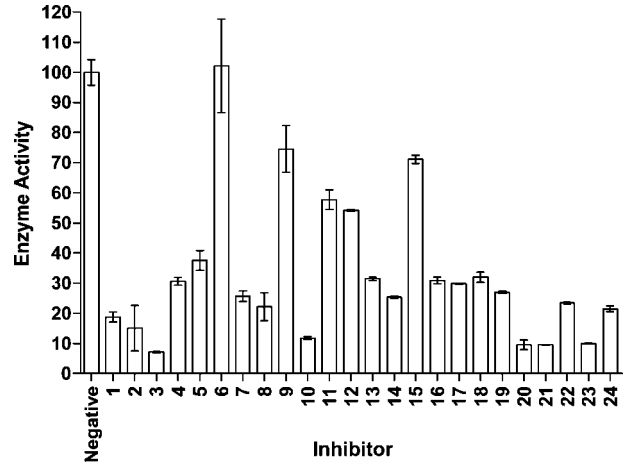

Figure 1. Inhibition (%) of WNV NS2B-NS3 protease by 10 μM tripeptide aldehydes (X-KKR-aldehyde), bearing an N-terminal cap X = 2-naphthoyl, **1**; cinnamoyl, **2**; phenacetyl, **3**; 2-pyrazinoyl, **4**; 2-indolyl, **5**; 1-naphthalenesulfonyl, **6**; 1-naphthoyl, **7**; biphenyl-4-carbonyl, **8**; 4-phenylcinnamoyl, **9**; 4-phenylphenylacetyl, **10**; 2-quinoxalinecarbonyl, **11**; 7-hydroxy-2-naphthoyl, **12**; chromone-2-carbonyl, **13**; 4-chlorocinnamoyl, **14**; 3,4-dimethoxycinnamoyl, **15**; 3-hydroxycinnamoyl, **16**; 4-dimethylaminocinnamoyl, **17**; 3-pyridylacryloyl, **18**; 4-pyridylacryloyl, **19**; 2-(7-methoxynaphyl)-propanoyl, **20**; 3-methoxyphenylacetyl, **21**; diphenylacetyl, **22**; 2-(3-benzylureido), **23**; benzyloxycarbonyl, **24**. Negative = no inhibitor.

Table 1. In Vitro Inhibition of WNV NS2B-NS3 Protease by Tripeptides (X-KKR-Aldehyde) Bearing an N-Terminal Cap, X

no.	X	IC_{50} (nM)	K_i (nM)
1	2-naphthoyl-	231	41
2	cinnamoyl-	580	104
3	phenacetyl-	51	9
10	4-phenyl-phenacetyl-	32	6
20	2-(7-methoxy-naphthyl)-propanoyl-	112	20
21	3-methoxy-phenacetyl-	60	11
23	2-(3-benzylureido)-	146	26
24	benzyloxycarbonyl-	222	40
25	benzoyl-	271	49
26	phenylpropanoyl-	454	81
27	phenoxyacetyl-	107	19
28	2-aminobenzoyl -	891	160

Table 2. In Vitro Inhibition of WNV NS2B-NS3 Protease by [Phenacetyl-P3-P2-P1-aldehyde] Compounds (P3-1 = Amino Acid)

no.	P3	P2	P1	IC_{50} (nM)	K_i (nM)
29	R	K	R	154	28
30	Orn	K	R	255	46
31	Cit	K	R	619	111
32	hR	K	R	245	44
33	K	R	R	325	58
34	K	Orn	R	73	13
35	K	Cit	R	11565	2073
36	K	hArg	R	297	53
37	K	K	W	25684	4604

containing arginine and lysine analogues were examined (compounds **29**−**36**; Table 2). The results suggest that a positive charge is required at P2 and P3 because citrulline (which is uncharged but isosteric with arginine) caused dramatic reductions in potency (230-fold at P2, compound **35**; 12-fold at P3, compound **31**). Also, there was a clear preference for lysine (**3**) at both P3 and P2 over either arginine (**29**, **33**) or homoarginine (**32**, **36**). Ornithine was well tolerated at P2 (**34**) but less so at P3 (**30**), while substitution of arginine at P1 by tryptophan was unfavorable (**37**). By comparison, the known (14) N-terminal capped tetrapeptide inhibitor, [Bz-(Nle)KRR-aldehyde], was much less potent in this work (IC_{50} 1.1 μM).

Enzyme Modeling Versus Crystal Structures. In early work on substrate/inhibitor binding to WNV NS2B/NS3 protease, we had used a homology model of this protease to guide site-directed mutagenesis studies.[11,12] In that work, we identified a small hydrophobic patch on the surface of the enzyme at Val-154 and Ile-155 in an otherwise polar and solvent-exposed substrate-binding cleft. We proposed that those residues contributed to an S4 pocket and were responsible for the observed preference of the protease for hydrophobic amino acids at P4 in substrates[11−13] and inhibitors.[15] A subsequently published crystal structure for WNV NS2B/NS3 protease[14] (PDB: 2fp7) supported the presence of this patch and also other residues (Leu87, Phe-85) contributed by the NS2B cofactor. However, the inhibitor in that crystal structure was bound in an unusual turn-like conformation, which was at odds with our observed structure−activity data and our site-directed mutagenesis.

The P4 norleucine residue for that inhibitor in the crystal structure was directed toward solvent, yet both literature[15] and our results have suggested that a bulky hydrophobic residue at the P4 position can substantially influence both substrate processing[13] and enzyme inhibition (Figure 1 and Table 1 above). We attributed this discrepancy to the fact that the crystal structure was determined for the protease crystallized at pH 7.5, rather than at pH 9.5 where catalysis is optimal, and thus might not reflect the relevant active conformation of the enzyme, which is virtually inactive at pH 7.5. While the higher pH might change the enzyme conformation to a more active form, it may also promote inhibitor/substrate binding perhaps by altering the electronic nature of the catalytic histidine, which should not be protonated above pH 7.5.

Alternatively, the binding mode of the inhibitor may be an artifact of crystallization. A third possibility is suggested by the finding of high B-factors in the crystal structure for a region of the NS2B cofactor that was reported[14] to bind both P2 and P3 substituents and that we had postulated to bind at the S4 subsite. This suggested to us that this putative S4 subsite may be flexible enough to accommodate larger residues and that the static crystal structure did not reflect this capacity. A subsequent pair of crystal structures for WNV NS2B/NS3 protease,[19] one of the H51A mutant (PDB code 2ggv) and one of the protease bound to a proteinaceous inhibitor (PDB: 2ijo), support this theory. The H51A mutant enzyme is misfolded and the NS2B cofactor was no longer in contact with the postulated S2−S4 region, but rather folded back onto itself on the other side of the enzyme, deviating from 2fp7 after residue W62. By contrast, the second inhibitor-bound structure (2ijo), despite minor differences, contains the same overall fold of NS2B and NS3 displayed in 2fp7.

Inhibitor-Enzyme Docking. Using ligand docking, we investigated how short tripeptide aldehydes may bind in the active site of the protease, using both the inhibitor-bound (2fp7) and partially unfolded (2ggv) forms of the protease, reasoning that these reflected two different conformational states of the S4 region of the enzyme. Figure 2 shows four of the molecular modeling results obtained when moderately large P4 (phenacetyl) and very large P4 (4-phenyl-phenacetyl) substitutents were added to the N-terminus of the optimal KKR-aldehyde inhibitor sequence. Phenacetyl-KKR-H fitted neatly into the enzyme active site defined by the 2fp7 crystal structure, with extensive hydrophobic contacts between the N-terminal capping residue and S4 (Figure 2A). In contrast, the same peptide aldehyde, while easily fitting into the enlarged S4 pocket of 2ggv, docks with unfavorable steric clashes in the S1 pocket, which in the crystal structure is greatly reduced in size (Figure 2B) due to movement of one wall of S1 defined by residues L149-I155. As observed previously for substrates,[13] some of the larger N-terminal substituents that had been predicted by enzyme activity and mutagenesis data to bind in an extended strand conformation, preferred to dock in turn-like conformations reminiscent of the crystal structure. For example, 4-phenylphenacetyl-KKR-H (Figure 2C) could not be docked easily in a strand-like conformation (typical of other proteases[25−27]) without significant steric clashes. Because the docking protocol in GOLD uses a rigid protein model, enforced inhibitor/protease complexes were subsequently relaxed via dynamics and minimization.[13] Relatively minor adjustments in the positions of the NS2B hairpin loop region sidechains allows the S4 subsite (Figure 2D) to "breathe" and accommodate larger P4 inhibitor groups.

These modeling results had suggested to us that neither of the two published crystal structures adequately describe the potential for ligand binding at S4 in the protease in solution. The structure−activity results (Figure 1, Table 1) observed herein reveal a capacity for the protease to accommodate quite large hydrophobic residues at the P4 position of substrates[13] and inhibitors. This is not predicted by the static crystal structures, which do not appear to reflect protein flexibility that can explain the importance of residues at P4 in ligand binding to the protease. This capacity, predicted by our modeling studies, could however be probed chemically with a panel of inhibitors X-KKR-H, where X was a hydrophobic capping residue of varying size and flexibility.

All the most potent inhibitors (Table 1, Figure 1) possessed slightly more flexible linker regions between the P4 carbonyl group and the terminal aromatic groups (e.g., phenacetyl) that most likely require less protein movement for optimal binding. All of the rigid naphthoyl-like N-terminal substituents had lower affinity than 2-naphthoyl-KKR-aldehyde, indicating that these generally bulkier analogues were approaching the limits of the allowable induced-fit space at S4. The genuine outliers were compounds with low inhibitor potency (e.g., **6**, **9**, **11**, **12**, **15**) that were either too bulky or too constrained to fit well at S4 or possessed unfavorable polar groups with poor complementarity for the protein surface.

Inhibitor Internalization In Living Cells. Cellular uptake was investigated using an analogue of aldehyde inhibitor **3**, where the phenacetyl group was substituted by the *ortho*-aminobenzoyl (2-Abz) fluorophore to give **28** (2-Abz-KKR-aldehyde, K_i 160 nM). Cos-1 cells were examined as these were of the same lineage as those used for the viral infectivity studies described ahead. Cultured cells were incubated with **28** for 1.5 h prior to examining uptake by live cell confocal microscopy (Figure 3B). Intracellular localization of **28** was seen as punctate vesicular fluorescence, indicating that the intact inhibitor had been taken up by cells. No fluorescence was observed in untreated cells (Figure 3A).

This surprising observation of cell permeability for the highly charged peptide inhibitor **28**, containing three side chains (Lys, Lys, Arg) that would all be positively charged at physiological pH, is counter-intuitive in that highly charged peptides do not normally cross the hydrophobic lipid bilayer membrane of a eukaryotic cell. However, the cellular entry of longer, much more highly charged, cationic peptides, such as in Tat, penetratin, or polyarginines, is now well-known to be an efficient method for promoting the cellular uptake of a wide range of molecular cargoes including drugs, peptides, proteins, and oligonucleotides,[28−34] reviewed elsewhere.[35] In those cases, the peptides featured between 5−12 positively charged amino acids

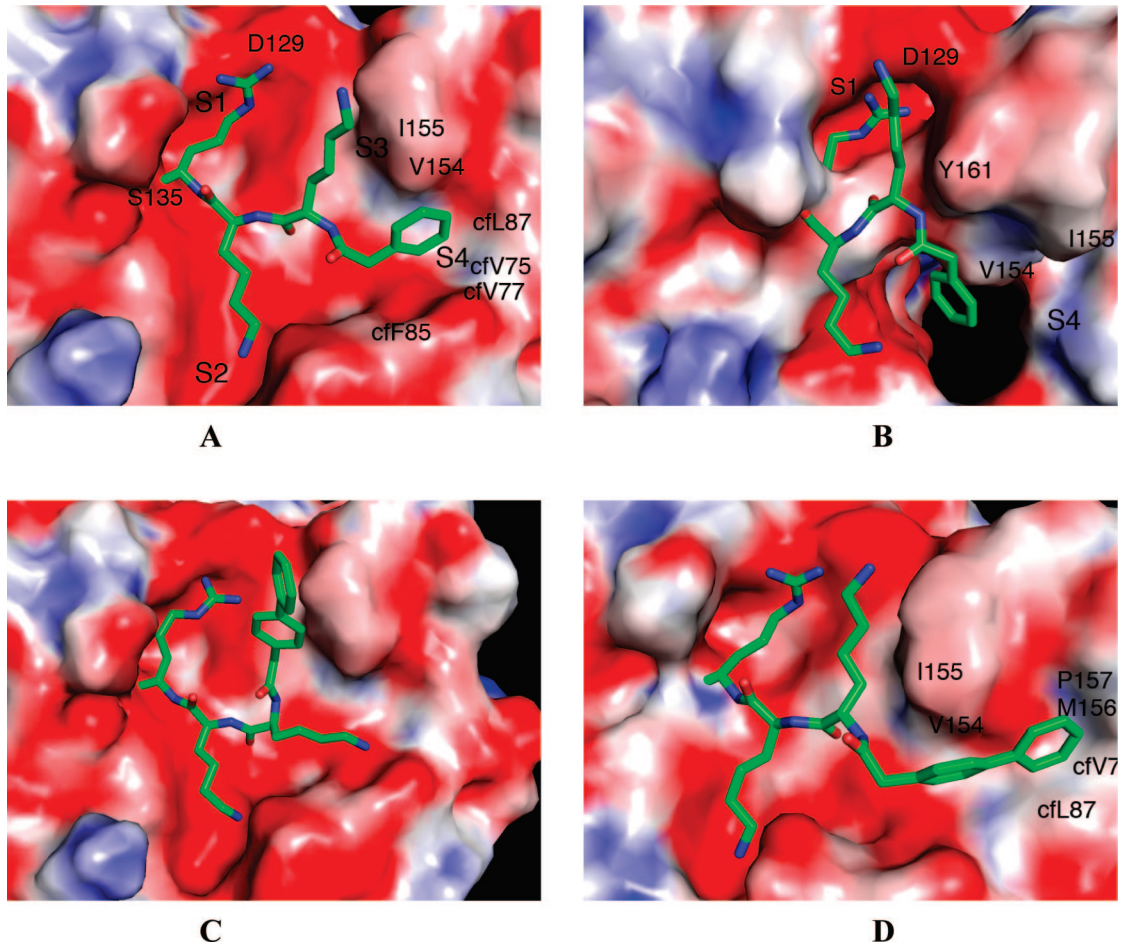

Figure 2. Inhibitors docked in protease crystal structures. Electrostatic surface of protease (Pymol) highlights acidic (red), basic (blue), and hydrophobic (white) regions with inhibitor as a stick model. For (**3**) in 2fp7 (A), the phenacetyl fits into the S4 pocket, whereas in 2ggv (B), the S1 pocket is partially occluded with S2−S4 enlarged due to absence of NS2B cofactor in this region. The bulkier (**10**) in 2fp7 (C) suggests ligand docking as a nonstandard turn conformation when no constraints on P3 and P4 were applied, and the S4 pocket is reduced in size; whereas docking in β-strand conformation (D) with subsequent simulated annealing enables some reorganization and enlarging of S4.

for efficient transport[29] unlike the observation here that three, and even two (Figure 3), cationic residues are sufficient to promote cellular uptake.

Previous studies have shown that highly charged cationic peptides such as polyarginine gain entry into cells via charged interactions with cell surface heparin sulfate (HS) followed by endocytosis of the cationic peptide/HS complexes.[36] Multiple steps are thought to be involved, including initial binding through hydrogen bond and charged interactions with cell surface heparin sulfate (HS), followed by endocytosis of the polyarginine/HS complex.[31] Glycosidase digestion of the HS within endocytic compartments is believed to release the peptide, which can then leak across the endocytic membrane into the cytosol.[31] The latter process is thought to be an active one, the polyarginine forming neutral complexes with phospholipids of the endocytic membrane and then crossing the membrane via a chemical gradient.[28,31,33]

The vesicular fluorescence seen in Figure 3B most likely represents inhibitor accumulation within endosomal compartments. To assess whether entry of inhibitor **28** into cells is dependent on positive charged side chain interactions with cell surface HS, we quantified its uptake by FACS analysis in the presence or absence of heparin (Figure 3C). Heparin treatment resulted in a 70% reduction in uptake of the inhibitor, supporting an important role for charged interactions in facilitating cell entry. In addition, we examined the effect of specific charge modifications to the inhibitor (Figure 3C) on cellular uptake. Ablation of a single positive charge at the P3 position was sufficient to reduce cellular uptake by as much as 80% (AbzK(Ac)KR-aldehyde), similar to the reduction seen following heparin treatment. A reduction of 80% was also seen for an inhibitor retaining only a single positive charge at the P1 position (AbzK(Ac)K(Ac)R-aldehyde), but only a 40% reduction in uptake was seen for the inhibitor in which the charge at the P2 position was removed (AbzKK(Ac)R-aldehyde). These results confirm an essential role of the charged side chains for efficient cellular uptake but also suggest that a specific topography of charge display may be necessary for efficient cellular entry.

Serum Stability Of Inhibitor. Because compound **28** was capable of entering cells, we sought to test such compounds for antiviral activity in cell culture. These assays involve the use of serum to culture cells, so we evaluated one of the potent aldehyde inhibitors (phenacetyl-KKR-aldehyde, **3**) for chemical stability in serum. This compound was found to be considerably more stable than the corresponding acid (phenacetyl-KKR-acid) in fetal calf serum, with no more than 10% degradation after 1−3 h at 37 °C compared to 100% degradation of its acidic counterpart (Figure 4). To our knowledge, mammalian proteases in blood do not readily recognize consecutive tri- (or di-) basic residues, although there are many enzymes that recognize a P1 basic residue. We found that μM concentrations of **3** either do not inhibit (e.g., factor Xa, urokinase) or inhibit only weakly (e.g., trypsin, plasmin) serine proteases that recognize a P1 basic residue (Supporting Information Table S1). We have previously

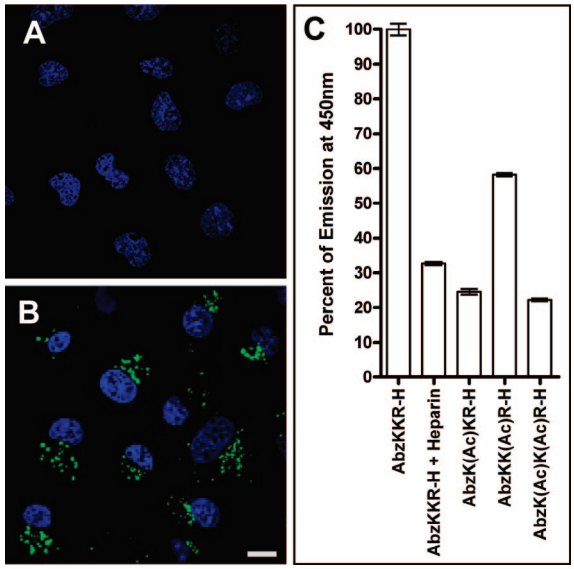

Figure 3. Uptake of fluorescent inhibitor into cos-1 cells. Inhibitor internalization was visualized by live cell confocal imaging: (A) treatment with buffer alone, (B) treatment with 500 μM of **28** (AbzKKR-aldehyde). Cell nuclei were counter-stained with Hoechst 33342. Bar = 10 μM. (C) Quantitation of cell uptake of AbzKKR-aldehyde ± heparin (1000 units/mL Heparin) and of charge-modified analogues of AbzKKR-aldehyde performed by FACS analysis and reported as % uptake relative to that of AbzKKR-aldehyde alone.

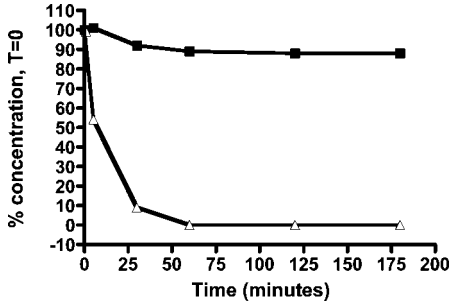

Figure 4. Serum stability of phenacetyl-KKR-aldehyde **3** (■) vs phenacetyl-KKR-OH (△). Vertical axis: normalized % peptide relative to concentration in supernatant at zero time.

shown that classic serine protease inhibitors (e.g., 100 μM PMSF, TLCK, leupeptin, benzamidine, FUT-175) that inhibit most mammalian serine proteases do not inhibit WNV NS2B-NS3pro.[11] The N-capping aromatic substituent and the C-terminal aldehyde in compounds like **3** limit endogenous proteases from truncating these compounds in blood, suggesting that the protease inhibitors could be used in antiviral studies with virus infected cells cultured in serum.

Antiviral Activity Of Phenacetyl-KKR-aldehyde (3) Against WNV (Kunjin Strain). Compound **3** was tested for antiviral activity in a plaque reduction assay. The inhibitor was assayed at concentrations ranging from 100 nM to 200 μM against WNV_{KUN}. Cells were infected with WNV_{KUN} in the presence of the compound and incubated at 37 °C with compound in the medium overlay. Plaque formation 48 h post infection (p.i.) was visualized by detection of viral antigen production by On Cell Western (Figure 5). Inhibitor activity was evidenced by a significant reduction in plaque size (Figure 5B) compared to control WNV_{KUN} plaques (Figure 5A), indicating inhibition of viral replication and consequent cell-to-cell spread of the virus. Quantification of plaque size was conducted in the presence of variable inhibitor concentrations

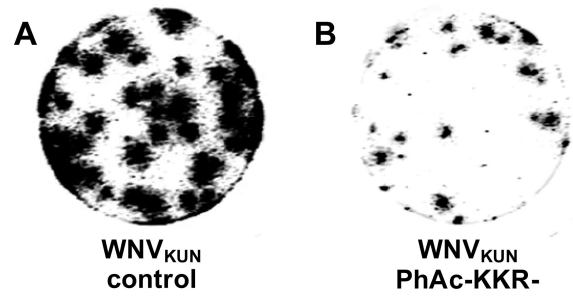

Figure 5. Antiviral activity of PhAc-KKR-aldehyde, **3**. Representative wells from inhibitor screen showing On Cell Western detection of plaque formation of WNV_{KUN} in Vero cells in the absence (A) versus presence (B) of 12.5 μM inhibitor.

and revealed an IC_{50} 1.6 μM. Plaque size reduction was not due to cytotoxicity because full cell viability measured in MTT assays was retained at inhibitor concentrations up to at least 400 μM.

The capacity of inhibitor **3**, PhAc-KKR-aldehyde, to inhibit viral replication suggests that the inhibitor is not only able to enter cells but is also able to leak across the endocytic membrane and localize in the infected cell within the viral induced convoluted membranes known to comprise the viral proteolytic compartment. The higher potency of the inhibitor **3** in vitro against the protease (K_i 9 nM) versus the cell based antiviral assay (IC_{50} 1.6 μM) most likely reflects the relative inefficiencies of inhibitor trafficking across multiple cellular membranes. Peptides can also trigger immunological responses, although peptides of this size tend not to be particularly immunogenic. Despite these additional challenges for further inhibitor optimization, these findings suggest that even substrate-based analogues may be useful antiviral probes for monitoring WNV replication and, due to substrate similarity, also the replication of other flaviviruses.

Conclusions

There is no effective treatment for WNV or other flavivirus infections, and attempts to develop inhibitors of flavivirus proteases with antiviral activity have so far been unsuccessful. This paper has described rationally designed small molecules that potently inhibit WNV protease. Even a tripeptide sequence, capped at the C-terminus by aldehyde and at the N-terminus by a flexible hydrophobic group, was sufficient to confer potent inhibition of the protease (Tables 1 and 2). The compounds were inhibitors at nM concentrations and exhibited reversible competitive kinetics, indicating that they target the substrate-binding active site of the protease. They were significantly more potent inhibitors of WNV protease than hexa- and tetra-peptide aldehydes examined previously by us and others.[11,15] The protease had a preference for inhibitors with Arg at P1, Lys at P2, and Lys at P3 (Table 2), the same as that observed for corresponding tripeptide substrates.[13] This supports a common binding mode for inhibitor and substrate with the same amino acids. The preference for Lys over Arg at P2 is a feature of substrate recognition by WNV protease, whereas the Dengue protease prefers Arg over Lys at P2.[13]

Structure−activity data show an important influence of P4 in the inhibitors, variations to the nonpeptidic N-terminal cap resulting in a 200-fold range of inhibitor potencies (Table 1, Figure 1, and unpublished). This suggests that the N-terminal cap interacts with protease residues in solution, and this is supported by a requirement of at least some flexibility at this position in order to obtain maximal inhibitory potency. Modeling

studies predicted that the N-terminal capping group might exploit space and hydrogen-bonding partners at the S4 position in the solution conformation of the protease. This contrasts with solid state crystal structure data,[14] which infers that capping groups would only protrude into surrounding solvent. Modeling also suggested that nonpeptidic fragments at P1 can potentially fit into the deep hydrophobic S1 groove of the enzyme, although tryptophan at P1 led to inactive inhibitors. A more fruitful direction might be to replace Arg/Lys residues with hydrophobic amino acid mimetics[37] and then remove the electrophilic (aldehyde) isostere. This has been the trend for other serine protease inhibitors where electrophilic isosteres are no longer needed for potent inhibition.[8,9]

Our finding that fluorescent inhibitor **28** (Abz-KKR-aldehyde), containing three positively charged residues, was taken up by cells and that this uptake was inhibited by heparin or by reducing the inhibitor charged state through acetylating either lysine side chain, strongly supports an endocytic uptake mechanism. The cell permeability of peptides with just two or three cationic side chains is surprising given previous findings that suggest poor cellular uptake of cationic peptides with less than five residues and of peptides with cationic residues other than arginine.[29] Its accumulation in vesicular compartments (Figure 3B) and long-term stability at 37 °C in serum (Figure 4) prompted us to evaluate antiviral activity for the more potent inhibitor analogue **3** in a plaque formation assay. The resulting antiviral activity (Figure 5) despite substantial peptide character suggests that such substrate analogues may be valuable probes for studying WNV replication and WNV protease action in living cells.

The finding that potent, competitive substrate-based inhibitors of this protease in vitro can penetrate cell membranes, despite being highly charged, and also inhibit replication of West Nile virus, is one of the first inhibitor-based validations of WNV protease as a prospective target for anti-WNV therapy. The results may signal a new means of transporting drugs/agents of low bioavailability across membranes and presented a new approach that may be useful for inhibiting other flavivirus proteases (dengue, yellow fever, Japanese encephalitis, tick-borne encephalitis, etc) which currently place up to three billion people worldwide at risk of infection.

Experimental Methods

Chemical Synthesis. Protected amino acids and resins were obtained from Auspep, Novabiochem, and PepChem. TFA, piperidine, DIPEA, DCM, and DMF (peptide synthesis grade) were purchased from Auspep. All other materials were reagent grade unless otherwise stated. Crude peptides were purified by reverse-phase HPLC on a Vydac C18, 10−15 mm, 300 Å, 50 mm × 250 mm) column, using a gradient mixture of solvent (A) 0.1%TFA/water and (B) 0.1%TFA/10%water/90%acetonitrile. Analytical HPLC was performed on a Waters system equipped with a 717 Plus autosampler, 660 controller and a 996 photodiode array detector, using a reverse-phase Phenomenex Luna C18, 5 mm, 100 Å, 250 mm × 4.6 mm column. Purified peptides were characterized by analytical HPLC (linear gradient 0−100% B over 30 min), mass spectrometry, and NMR (Supporting Information). The molecular weight of the peptides (1 mg/mL) was determined by electrospray mass spectrometry on a Micromass LCT mass spectrometer. ^{1}H NMR spectra were recorded on samples containing 4 mM peptide in DMSO-d_6 (550 μL) on Bruker Avance 600 spectrometer at 298 K.

The chromogenic substrate Ac-LKKR-pNA was prepared by the method of Abbenante et al.[38] Aldehyde inhibitors were prepared by the method of Siev et al. using Fmoc protocols,[39] and were rechecked for racemization by ^{1}H NMR spectroscopy immediately prior to assay.

Modeling Inhibitor-NS2B/NS3 Interactions. The original crystal structure[14] of West Nile virus NS2B/NS3 protease (PDB code: 2fp7), the H51A mutant (PDB code: 2ggv),[19] and the BPTI-complexed protein (PDB code: 2ijo)[19] were prepared for docking by removing the bound ligands and water molecules and adding protons using InsightII (Version 2000; Accelrys Inc.). Aldehyde inhibitors were assembled using the Biopolymer and Sketcher modules in InsightII and minimized using Discover. All docking experiments were performed using GOLD v3.1[40] on Red Hat Enterprise 4 Linux workstations, and docked conformations of ligands were analyzed using Pymol[41] or InsightII. Electrostatic surfaces were generated using the APBS plugin in Pymol.[42,43] Docking runs were performed with the aldehyde carbonyl carbon converted from sp2 to sp3 geometry and covalently linked to the protease. A hydrogen bonding and distance constraint protocol previously described[13] to allow the inhibitors to adequately sample β-strand conformations was used to align the inhibitors within the active site. No constraints on the position of P3 and P4 side chains were used. For the inhibitors with larger N-terminal capping residues (e.g., 2-naphthoyl, 4-phenylphenacetyl), docking poses with the cap directed out of the active site toward solvent were sometimes observed. In these cases, dockings were repeated with soft distance constraints restricting the substituents to the vicinity of S4. The initial high energy docked poses were subsequently optimized using a molecular dynamics and minimization protocol using Discover (Accelrys) as described.[13]

In Vitro Enzyme Inhibition. Inhibition of recombinant WNV protease activity was measured at pH 9.5 as described.[11] The recombinant WNV protease consisted of the essential 40 amino acid cofactor domain of NS2B linked to the N-terminal 184 amino acids of NS3 by a flexible nonapeptide (Gly4-Ser-Gly4) generated as reported.[11] The assay was conducted in 96-well plates with a final volume of 200 μL. Recombinant WNV protease and aldehyde inhibitors were mixed with assay buffer (50 mM glycine-NaOH, 1 mM CHAPs, 30% glycerol) to give a final enzyme concentration of 25 nM and eight concentrations of inhibitor, each in triplicate, ranging from 20 μM to 1 nM. After preincubation of enzyme with inhibitor in separate wells (10 min at 37 °C), catalysis was initiated by adding substrate AcLKKR-pNA to a final concentration of 250 μM. Cleavage of the pNA chromophore from substrate produced a color change monitored at 405 nm. Optical density was measured every 30 s for 10 min by a Spectromax 250 reader, and K_i values were determined by Graphpad Prism.[41]

Serum Stability of Inhibitor. A stock solution (250 μL) of aldehyde inhibitor (Phenacetyl-KKR-aldehyde, 37 mM) or control peptide acid (Phenacetyl-KKR-acid, 33 mM) was added to 4750 μL of either water (negative control) or filtered fetal calf serum (Invitrogen). The serum was not heat-inactivated. Immediately after addition (T= 0) and at 5 min, 30 min, 1 h, 2 h, and 3 h time intervals, 500 μL was removed and protein precipitated with acetonitrile (1500 μL). Samples were centrifuged (2500 rpm, 5 min) and supernatant was analyzed by mass spectrometry and analytical HPLC for the peptide.

Cells and Virus Preparation. Vero and Cos-1 cells were maintained in Dulbecco's modified Eagle media (DMEM) supplemented with 4% fetal bovine serum (FBS) in 5% CO_2 at 37 °C. Working stocks of West Nile virus, Kunjin strain (WNV_{KUN}) were prepared as media harvests from infected Vero cells and stored at −80 °C. Compounds were dissolved in distilled water and stocks stored at −80 °C. Inhibitors were freshly prepared from stocks and filter sterilized before testing.

MTT Cell Viability Assay. MTT [3-(4,5-dimethylthiazol-2-yl)2,5-diphenyl tetrazolium bromide] cell viability assays were performed to determine cytotoxicity of compounds. Vero cells (4×10^4 in 100 μL media) were seeded in a 96-well plate and incubated to 90% confluency for ∼12 h. Culture media was substituted by fresh media containing compounds at concentrations from 5 nM to 400 μM or control media with or without DMSO. At 72 h post incubation, 10 μL of MTT (5 mg/mL PBS) was added and cells incubated at 37 °C. After 3.5 h, 100 μL of 0.04 M HCl in isopropanol was added and plates kept in the dark and gently

swirled for 4 h at room temperature (RT). A microtiter plate reader (Molecular Devices SpectraMax250) was used to record absorbance at 550 nm, from which CC_{50} values were estimated. Assays were performed in duplicate.

Confocal Microscopy. Cos-1 cells were grown on coverslips in 24 well-plates overnight at a density of 5×10^5/mL. Inhibitor **28** (2Abz-KKR-aldehyde), containing a 2-aminobenzoyl fluorophore (Abz), was diluted in phosphate-buffered saline (PBS) or Hank's buffered salt solution (HBSS), applied to cells and incubated for 1.5 h in the dark in a humid chamber at 37 °C/5%CO_2. Mock cells were treated with PBS or HBSS only. Nuclear counterstaining by Hoechst 33342 (0.4 mg/mL) was performed for 15 min at 37 °C/5%CO_2 followed by two washes with PBS. Coverslips were then mounted on slides using CyGEL (Biostatus) to allow cell sustainability but reduce cell movement, and cells were immediately imaged using a Zeiss LSM 510 Meta confocal microscope and Zeiss software.

FACS Analysis of Cellular Uptake of Inhibitors. Cellular uptake of aldehyde inhibitors was quantified by fluorescent-activated cell sorting (FACS). BHK cells (1×10^6) in 1 mL of OPTI-MEM (Gibco) containing 3% FCS was added to each well of a 6-well plate and incubated at 37 °C for 2 h to allow cells to attach. Fluorescent aldehyde inhibitors ± 1000 units/mL Heparin were then added to give a final concentration of 1 mM and the same volume of filter sterilized H_2O was added to the negative control. Cells were incubated at 37 °C for 1.5 h to allow entry of fluorescent aldehyde inhibitors. Media was removed and cells were washed with Hanks' solution (Sigma) and then harvested using 250 μL of 0.05% trypsin-versene for 5 min at 37 °C. One mL of media was added before placing cells in 1.5 mL microfuge tubes. Cells were pelleted by centrifugation at 2000 rpm for 2 min and washed three times by resuspension in 1 mL of Hanks' solution. Fluorescence was measured for 10000 cells (excitation 315 nm, emission 450 nm) in the BD LDSR II analyzer. Mean fluorescence and standard error were calculated.

Immuno-Plaque Assay. The antiviral effects of compounds were assayed by On Cell Westerns as described below. Vero cells (4×10^4 in 100 μL media) were seeded in a 96-well plate and incubated until 90% confluent (approximately 12 h). Media was removed, and monolayers were washed once with PBS and then with serum-free (SF) media. Virus and compounds were separately diluted in SF media. Cells were coincubated with compound concentrations ranging from 100 nM to 200 μM with WNV_{KUN} at a multiplicity of infection (moi) of 0.04 at 37 °C/5% CO_2. Mock-infected cells were incubated with SF media only. After 2 h, the media was overlaid with M199-media containing 3% FBS and 1.2% carboxymethyl cellulose (final concentration), followed by further incubation for 48 h. Cells were fixed with 4% *para*-formaldehyde for 20 min at RT and permeabilized with three washes in PBS containing 0.1% Triton-X100 for 5 min. Skim milk powder blocking solution (5% MP in PBS) was added and incubated at 4 °C for 4 h. An anti-WNV_{KUN} NS1 mouse monoclonal antibody (0.24 mg/well) was substituted and further incubated at 4 °C overnight. The monolayer was washed 5 × 5 min with PBS containing 0.1% Tween 20. AlexaFluor680 conjugated rabbit antimouse IgG (0.2 mg/well) was added and incubated at RT in the dark for 1 h. The plates were washed as described above and then briefly dried in the dark. 96-well plates were scanned and analyzed using the LI-COR Biosciences Odyssey Infrared Imaging System and application software. Plaque sizes were measured as infrared signals in counts per mm^2. Ten plaques per well were averaged, IC_{50} values derived from dose−response curves, and compounds tested in duplicate.

Acknowledgment. We thank the National Health and Medical Research Council and the Australian Research Council for research support, and the ARC for a Federation Fellowship to D.P.F.

Supporting Information Available: . Structures of the N-terminal capping groups used in this study, experimental methods, characterization data for compounds **1**−**40**, as well as sample NMR, HPLC, and serine protease inhibition data. This material is available free of charge via the Internet at http://pubs.acs.org.

References

(1) Merianos, A. Surveillance and response to disease emergence. *Curr. Top. Microbiol. Immunol.* **2007**, *315*, 477–509.
(2) Centers for Disease Control and Prevention Division of Vector-Borne Infectious Disease; West Nile Virus (http://www.cdc.gov/ncidod/dvbid/westnile/); Dengue (http://www.cdc.gov/ncidod/dvbid/dengue/index.htm); World Health Organisation, Yellow Fever (http://www.who.int/mediacentre/news/releases/2007/pr23/en/index.html); Japanese Encephalitis (http://www.path.org/projects/JE_in_depth.php).
(3) Kramer, L. D.; Styer, L. M.; Ebel, G. D. A global perspective on the epidemiology of West Nile virus. *Annu. Rev. Entomol.* **2008**, *53*, 61–81.
(4) Ferguson, N. M.; Fraser, C.; Donnelly, C. A.; Ghani, A. C.; Anderson, R. M. Public health. Public health risk from the avian H5N1 influenza epidemic. *Science* **2004**, *304*, 968–969.
(5) Petersen, L. R.; Roehrig, J. T. West Nile virus: a reemerging global pathogen. *Emerg. Infect. Dis.* **2001**, *7*, 611–614.
(6) Bazan, J. F.; Fletterick, R. J. Detection of a trypsin-like serine protease domain in flaviviruses and pestiviruses. *Virology* **1989**, *171*, 637–639.
(7) Chambers, T. J.; Weir, R. C.; Grakoui, A.; McCourt, D. W.; Bazan, J. F.; Fletterick, R. J.; Rice, C. M. Evidence that the N-terminal domain of nonstructural protein NS3 from yellow fever virus is a serine protease responsible for site-specific cleavages in the viral polyprotein. *Proc. Natl. Acad. Sci. U.S.A.* **1990**, *87*, 8898–9802.
(8) Leung, D.; Abbenante, G.; Fairlie, D. P. Protease inhibitors: current status and future prospects. *J. Med. Chem.* **2000**, *43*, 305–341.
(9) Abbenante, G.; Fairlie, D. P. Protease inhibitors in the clinic. *Med. Chem.* **2005**, *1*, 71–104.
(10) Falgout, B.; Pethel, M.; Zhang, Y. M.; Lai, C. J. Both nonstructural proteins NS2b and NS3 are required for the proteolytic processing of dengue virus nonstructural proteins. *J. Virol.* **1991**, *65*, 2467–2475.
(11) Nall, T. A.; Chappell, K. J.; Stoermer, M. J.; Fang, N. X.; Tyndall, J. D. A.; Young, P. R.; Fairlie, D. P. Enzymatic characterization and homology model of a catalytically active recombinant West Nile virus NS3 protease. *J. Biol. Chem.* **2004**, *279*, 48535–48542.
(12) Chappell, K. J.; Nall, T. A.; Stoermer, M. J.; Fang, N. X.; Tyndall, J. D. A.; Fairlie, D. P.; Young, P. R. Site-directed mutagenesis and kinetic studies of the West Nile virus NS3 protease identify key enzyme−substrate interactions. *J. Biol. Chem.* **2005**, *280*, 2896–2903.
(13) Chappell, K. J.; Stoermer, M. J. R.; Fairlie, D. P.; Young, P. Insights to substrate binding and processing by West Nile virus NS3 protease through combined modeling, protease mutagenesis, and kinetic studies. *J. Biol. Chem.* **2006**, *281*, 38448–38458.
(14) Erbel, P.; Schiering, N.; D'Arcy, A.; Renatus, M.; Kroemer, M.; Lim, S. P.; Yin, Z.; Keller, T. H.; Vasudevan, S. G.; Hommel, U. Structural basis for the activation of flaviviral NS3 proteases from Dengue and West Nile virus. *Nat. Struct. Mol. Biol.* **2006**, *13*, 372–373.
(15) Knox, J. E.; Ma, N. L.; Yin, Z.; Patel, S. J.; Wang, W. L.; Chan, W. L.; Ranga Rao, K. R.; Wang, G.; Ngew, X.; Patel, V.; Beer, D.; Lim, S. P.; Vasudevan, S. G.; Keller, T. H. Peptide Inhibitors of West Nile NS3 Protease: SAR Study of Tetrapeptide Aldehyde Inhibitors. *J. Med. Chem.* **2006**, *49*, 6585–6590.
(16) Shiryaev, S. A.; Kozlov, I. A.; Ratnikov, B. I.; Smith, J. W.; Lebl, M.; Strongin, A. Y. Cleavage preference distinguishes the two-component NS2B-NS3 serine proteinases of Dengue and West Nile viruses. *Biochem. J.* **2007**, *401*, 743–752.
(17) Shiryaev, S. A.; Ratnikov, B. I.; Aleshin, A. E.; Kozlov, I. A.; Nelson, N. A.; Lebl, M.; Smith, J. W.; Liddington, R. C.; Strongin, A. Y. Switching the substrate specificity of the two-component NS2B-NS3 flavivirus proteinase by structure-based mutagenesis. *J Virol.* **2007**, *81*, 4501–4509.
(18) Chappell, K. J.; Stoermer, M. J.; Fairlie, D. P.; Young, P. R. Generation and characterization of proteolytically active and highly stable truncated and full-length recombinant West Nile virus NS3. *Protein Expression Purif.* **2007**, *53*, 87–96.
(19) Aleshin, A. E.; Shiryaev, S. A.; Strongin, A. Y.; Liddington, R. C. Structural evidence for regulation and specificity of flaviviral proteases and evolution of the Flaviviridae fold. *Protein Sci.* **2007**, *16*, 795–806.
(20) Bera, A. K.; Kuhn, R. J.; Smith, J. L. Functional Characterization of cis and trans Activity of the Flavivirus NS2B-NS3 Protease. *J. Biol. Chem.* **2007**, *282*, 12883–12892.
(21) Shiryaev, S. A.; Ratnikov, B. I.; Chekanov, A. V.; Sikora, S.; Rozanov, D. V.; Godzik, A.; Wang, J.; Smith, J. W.; Huang, Z.; Lindberg, I.; Samuel, M. A.; Diamond, M. S.; Strongin, A. Y. Cleavage targets and the D-arginine-based inhibitors of the West Nile virus NS3 processing proteinase. *Biochem. J.* **2006**, *393*, 503–511.

(22) Ganesh, V. K.; Muller, N.; Judge, K.; Luan, C. H.; Padmanabhan, R.; Murthy, K. H. M. Identification and characterization of nonsubstrate based inhibitors of the essential Dengue and West Nile virus proteases. *Bioorg. Med. Chem.* **2005**, *13*, 257–264.

(23) Leung, D.; Schroder, K.; White, H.; Fang, N. X.; Stoermer, M. J.; Abbenante, G.; Martin, J. L.; Young, P. R.; Fairlie, D. P. Activity of recombinant dengue 2 virus NS3 protease in the presence of a truncated NS2B cofactor, small peptide substrates, and inhibitors. *J. Biol. Chem.* **2001**, *276*, 45762–45771.

(24) Li, J.; Lim, S. P.; Beer, D.; Patel, V.; Wen, D.; Tumanut, C.; Tully, D. C.; Williams, J. A.; Jiricek, J.; Priestle, J. P.; Harris, J. L.; Vasudevan, S. G. Functional profiling of recombinant NS3 proteases from all four serotypes of dengue virus using tetrapeptide and octapeptide substrate libraries. *J. Biol. Chem.* **2006**, *280*, 28766–28774.

(25) Tyndall, J.; Fairlie, D. P. Conformational Homogeneity In Molecular Recognition By Proteolytic Enzymes. *J. Mol. Recognit.* **1999**, *12*, 363–370.

(26) Fairlie, D. P.; Tyndall, J. D. A.; Reid, R. C.; Wong, A. K.; Abbenante, G.; Scanlon, M. J.; March, D. R.; Bergman, D. A.; Chai, C. L. L.; Burkett, B. A. Conformational Selection Of Inhibitors and Substrates By Proteolytic Enzymes: Implications for Drug Design and Polypeptide Processing. *J. Med. Chem.* **2000**, *43*, 1271–1281.

(27) Tyndall, J. D. A.; Nall, T.; Fairlie, D. P. Proteases Universally Recognize Beta Strands In Their Active Sites. *Chem. Rev.* **2005**, *105*, 973–1000.

(28) Rothbard, J. B.; Garlington, S.; Lin, Q.; Kirschberg, T.; Kreider, E.; McGrane, P. L.; Wender, P. A.; Khavari, P. A. Conjugation of arginine oligomers to cyclosporin A facilitates topical delivery and inhibition of inflammation. *Nat Med.* **2000**, *6*, 1253–1257.

(29) Mitchell, D. J.; Kim, D. T.; Steinman, L.; Fathman, C. G; Rothbard, J. B. Polyarginine enters cells more efficiently than other polycationic homopolymers. *J. Pept. Res.* **2000**, *56*, 318–325.

(30) Samuel, B. U.; Hearn, B.; Mack, D.; Wender, P.; Rothbard, J.; Kirisits, M. J.; Mui, E; Wernimont, S; Roberts, C. W.; Muench, S. P.; Rice, D. W.; Prigge, S. T.; Law, A. B.; McLeod, R. Delivery of antimicrobials into parasites. *Proc. Natl. Acad. Sci. U.S.A.* **2003**, *100*, 14281–14286.

(31) Rothbard, J. B.; Jessop, T. C.; Lewis, R. S.; Murray, B. A.; Wender, P. A. Role of membrane potential and hydrogen bonding in the mechanism of translocation of guanidinium-rich peptides into cells. *J. Am. Chem. Soc.* **2004**, *126*, 9506–9507.

(32) Thorén, P. E.; Persson, D.; Esbjörner, E. K.; Goksör, M.; Lincoln, P.; Nordén, B. Membrane binding and translocation of cell-penetrating peptides. *Biochemistry* **2004**, *43*, 3471–3489.

(33) Rothbard, J. B.; Jessop, T. C.; Wender, P. A. Adaptive translocation: the role of hydrogen bonding and membrane potential in the uptake of guanidinium-rich transporters into cells. *Adv. Drug. Delivery Rev.* **2005**, *57*, 495–504.

(34) Zorko, M.; Langel, U. Cell-penetrating peptides: mechanism and kinetics of cargo delivery. *Adv. Drug. Delivery Rev.* **2005**, *57*, 529–545.

(35) Fuchs, S. M.; Raines, R. T. Internalization of cationic peptides: the road less (or more?) traveled. *Cell. Mol. Life Sci.* **2006**, *63*, 1819–1822.

(36) Fuchs, S. M.; Raines, R. T. Pathway for polyarginine entry into mammalian cells. *Biochemistry* **2004**, *43*, 2438–2444.

(37) Peterlin-Masic, L.; Kikelj, D. Arginine Mimetics. *Tetrahedron* **2001**, *57*, 7073–7105.

(38) Abbenante, G.; Leung, D.; Bond, T.; Fairlie, D. P. An efficient Fmoc strategy for the rapid synthesis of peptide *para*-nitroanilides. *Lett. Pept. Sci.* **2000**, *7*, 347–351.

(39) Siev, D. V.; Semple, J. E. Novel hydrazino-carbonyl-amino-methylated polystyrene (HCAM) resin methodology for the synthesis of P1-aldehyde protease inhibitor candidates. *Org. Lett.* **2000**, *2*, 19–22.

(40) Jones, G.; Willett, P.; Glen, R. C.; Leach, A. R.; Taylor, R. Development and validation of a genetic algorithm for flexible docking. *J. Mol. Biol.* **1997**, *267*, 727–748.

(41) DeLano, W. L. *PyMOL Molecular Graphics System*, DeLano Scientific LLC: San Carlos, CA; http://www.pymol.org.

(42) Baker, N. A.; Sept, D.; Joseph, S.; Holst, M. J.; McCammon, J. A. Electrostatics of nanosystems: application to microtubules and the ribosome. *Proc. Natl. Acad. Sci. U.S.A.* **2001**, *98*, 10037–10041.

(43) Cheng, Y.; Prusoff, W. H. Relationship between the inhibition constant (K1) and the concentration of inhibitor which causes 50% inhibition (I50) of an enzymatic reaction. *Biochem. Pharmacol.* **1973**, *22*, 3099–3108.

JM800503Y